

Formation and Redox Reactivity of Osmium(II) Thionitrosyl Complexes

El-Sayed El-Samanody,^{†,‡} Konstantinos D. Demadis,[§] Laurie A. Gallagher,[†] Thomas J. Meyer,^{*,†} and Peter S. White[†]

Department of Chemistry, Venable and Kenan Laboratories, CB 3290, University of North Carolina at Chapel Hill, Chapel Hill, North Carolina 27599-3290, and Nalco Chemical Company, Global Water Research, One Nalco Center, Naperville, Illinois 60563-1198

Received December 18, 1998

Reaction between $[\text{Os}^{\text{VI}}(\text{tpm})(\text{Cl})_2(\text{N})](\text{PF}_6)$ (tpm = tris(1-pyrazolyl)methane) (**1**) or $\text{Os}^{\text{VI}}(\text{Tp})(\text{Cl})_2(\text{N})$ (Tp = hydrotris(1-pyrazolyl)borate anion) (**2**) and $\text{CS}_2 + \text{N}_3^-$ in acetone gives the corresponding thionitrosyl complexes, $-\text{SCN}$, and N_2 . There is an extensive reactivity chemistry of the thionitrosyl group in $[\text{Os}^{\text{II}}(\text{tpm})(\text{Cl})_2(\text{NS})](\text{PF}_6)$ (**3b**). Reaction between **3b** and PPh_3 occurs with S-atom transfer to give $[\text{Os}^{\text{IV}}(\text{tpm})(\text{Cl})_2(\text{NPPH}_3)]^+$ and $\text{S}=\text{PPh}_3$. **3b** undergoes chemical or electrochemical reduction to give the corresponding Os^{II} ammine complex and H_2S . O-atom transfer from $\text{O}=\text{NMe}_3$ to **3b** occurs to give $\text{Os}^{\text{III}}(\text{tpm})(\text{Cl})_2(\text{NSO})$. Competitive NO^+/NS^+ exchange and S^{2-} transfer occur in the reaction between $[\text{Os}^{\text{II}}(\text{tpm})(\text{Cl})_2(\text{NS})](\text{BF}_4)$ (**3c**) and NO^+ to give a mixture of $[\text{Os}^{\text{VI}}(\text{tpm})(\text{Cl})_2(\text{N})]^+$ and $[\text{Os}^{\text{II}}(\text{tpm})(\text{Cl})_2(\text{NO})]^+$.

Introduction

There is an extensive transition metal nitrosyl chemistry with many examples and a variety of reactions based on the coordinated ligand.¹ There is also a related thionitrosyl chemistry. Although less well developed, it is extensive with well-defined examples for Cr,^{2a,b} Mo,^{2c} W,^{2c} Mn,^{2b} Re,^{3a–d} Tc,^{3c–j} Ru,^{4a–c} and Os.^{4d–h} The synthetic aspects of thionitrosyl chemistry have been described in various reviews.⁵ Recently,

we reported a new procedure for the preparation of Os^{II} thionitrosyl complexes based on a reaction between Os^{VI} nitrido complex and CS_2 in the presence of N_3^- .⁶

We report here an extension of the thionitrosyl synthetic chemistry to the preparation of $\text{Os}^{\text{II}}(\text{Tp})(\text{Cl})_2(\text{NS})$ (Tp is hydrotris(1-pyrazolyl)borate anion) and the existence of an extensive redox chemistry based on the NS ligand in $[\text{Os}^{\text{II}}(\text{tpm})(\text{Cl})_2(\text{NS})]^+$ (tpm is tris(1-pyrazolyl)methane). Ligand structures are illustrated in Figure 1.

A theme of interest was a comparison between the reactivities of the nitrosyl and thionitrosyl ligands. In relatively high oxidation state $d\pi^6$ Ru^{II} and Os^{II} nitrosyl complexes the electronic distribution at NO leaves the nitrogen atom relatively electron deficient.^{7a–e} Reactivity at the ligand is dominated by nucleophilic addition at the nitrogen atom of the nitrosyl. Reduction occurs at a level largely $\pi^*(\text{NO})$ in character.^{7g–i}

In the electronic distribution in related thionitrosyls the sulfur atom is electron deficient relative to nitrogen, potentially changing the site for nucleophilic attack.^{5a,c,7} The sulfur atom is also more amenable to redox change with the possibility existing for net reduction based on S-atom transfer and oxidation by sulfoxide formation.

* Corresponding author. E-mail: tjmeyer@email.unc.edu.

† University of North Carolina at Chapel Hill.

‡ On leave from the Department of Chemistry, Menoufia University, Egypt.

§ Nalco Chemical Company

- (1) Richter-Addo, G. B.; Legzdins, P. *Metal Nitrosyls*; Oxford University Press: New York, 1992, and references therein.
- (2) (a) Herrmann, W. A.; Rohrmann, J.; Noeth, H.; Narula, C. K.; Bernal, I.; Draux, M. *J. Organomet. Chem.* **1985**, *284*, 189. (b) Beron, K.; Steinke, G.; Mews, R. *Chem. Ber.* **1989**, *122*, 1613. (c) Bevan, P. C.; Chatt, J.; Dilworth, J. R.; Henderson, R. A.; Leigh, G. J. *J. Chem. Soc., Dalton Trans.* **1982**, 821. (d) Seth, J.; Gupta, M.; Agarwala, U. C. *Bull. Chem. Soc. Jpn.* **1988**, *61*, 1446.
- (3) (a) Mews, R.; Liu, C. S. *Angew. Chem., Int. Ed. Engl.* **1983**, *22*, 158. (b) Anhauser, J.; Siddiqi, Z. A.; Roesky, H. W.; Bats, J. W.; Elerman, Y. Z. *Naturforsch.* **1985**, *40B*, 740. (c) Abram, U.; Ritter, S. Z. *Anorg. Allg. Chem.* **1994**, *620*, 1223. (d) Huebener, R.; Abram, U.; Strähle, J. *Inorg. Chim. Acta* **1994**, *216*, 223. (e) Abram, U.; Huebener, R.; Wollert, R.; Kirmse, R.; Hiller, W. *Inorg. Chim. Acta* **1993**, *206*, 9. (f) Baldas, J.; Colmanet, S. E.; Williams, G. A. *Aust. J. Chem.* **1991**, *44*, 1125. (g) Hiller, W.; Huebener, R.; Lorenz, B.; Kaden, L.; Findeisen, M.; Stach, J.; Abram, U. *Inorg. Chim. Acta* **1991**, *181*, 161. (h) Lu, J.; Clarke, M. J. *Inorg. Chem.* **1990**, *29*, 4123. (i) Kaden, L.; Lorenz, B.; Kirmse, R.; Stach, J.; Behm, H.; Beurskens, P. T.; Abram, U. *Inorg. Chim. Acta* **1990**, *169*, 43. (j) Abram, U.; Kirmse, R.; Koehler, K.; Lorenz, B.; Kaden, L. *Inorg. Chim. Acta* **1987**, *129*, 15.
- (4) (a) Bats, J. W.; Pandey, K. K.; Roesky, H. W. *J. Chem. Soc., Dalton Trans.* **1984**, 2081. (b) Udupa, K. N.; Jain, K. C.; Khan, M. I.; Agarwala, U. C. *Inorg. Chim. Acta* **1982**, *74*, 191. (c) Willing, W.; Mueller, U.; Demant, U.; Dehnicke, K. Z. *Naturforsch.* **1986**, *41B*, 560. (d) Wright, M. J.; Griffith, W. P. *Trans. Met. Chem.* **1982**, *7*, 53. (e) Pandey, K. K.; Roesky, H. W.; Noltemeyer, M.; Sheldrick, G. M. *Z. Naturforsch.* **1984**, *39B*, 590. (f) Weber, R.; Mueller, U.; Dehnicke, K. Z. *Anorg. Allg. Chem.* **1983**, *504*, 13. (g) Weber, R.; Dehnicke, K. Z. *Naturforsch.* **1984**, *39B*, 262. (h) Roesky, H. W.; Pandey, K. K.; Clegg, W.; Noltemeyer, M.; Sheldrick, G. M. *J. Chem. Soc., Dalton Trans.* **1984**, 719.

- (5) (a) Roesky, H. W.; Pandey, K. K. *Adv. Inorg. Radiochem.* **1983**, *26*, 337. (b) Kelly, P. F.; Woollins, J. D. *Polyhedron* **1986**, *5*, 606. (c) Chivers, T.; Edelmann, F. *Polyhedron* **1986**, *5*, 1661. (d) Johnson, B. F. G.; Haymore, B. L.; Dilworth, J. R. In *Comprehensive Coordination Chemistry*; Wilkinson, G., Ed.; Pergamon: New York, 1987; Vol. 2, p 119. (e) Pandey, K. K. *Prog. Inorg. Chem.* **1992**, *40*, 445.
- (6) (a) Demadis, K. D.; El-Samanody, E.-S.; Meyer, T. J.; White, P. S. *Inorg. Chem.* **1998**, *37*, 838. (b) Demadis, K. D.; Meyer, T. J.; White, P. S. *Inorg. Chem.* **1998**, *37*, 3610.
- (7) (a) Pandey, K. K. *J. Coord. Chem.* **1991**, *22*, 307. (b) Pandey, K. K.; Sharma, R. B.; Pandit, P. K. *Inorg. Chim. Acta* **1990**, *169*, 207. (c) Pandey, K. K.; Ahuja, S. R.; Goyal, M. *Indian J. Chem., Sect. A* **1985**, *24A*, 1059. (d) Bowden, W. L.; Little, W. F.; Meyer, T. J. *J. Am. Chem. Soc.* **1977**, *99*, 4340. (e) Bowden, W. L.; Little, W. F.; Meyer, T. J. *J. Am. Chem. Soc.* **1976**, *98*, 444. (f) Mehlhorn, A.; Fabian, J.; Gabriel, W.; Rosmus, P. *THEOCHEM* **1995**, *339*, 219. (g) Kersting, M.; Hoffmann, R. *Inorg. Chem.* **1990**, *29*, 279. (h) Karna, S. P.; Grein, F. *Chem. Phys.* **1986**, *109*, 35. (i) Callahan, R. W.; Brown, G. M.; Meyer, T. J. *J. Am. Chem. Soc.* **1975**, *97*, 894.

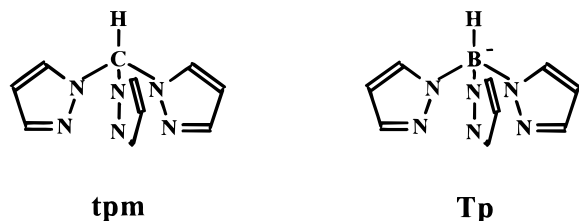


Figure 1. Ligand structures: tpm = tris(1-pyrazolyl) methane; Tp = hydrotris(1-pyrazolyl)borate anion.

Experimental Section

The following compounds and salts appear in this study: $[\text{Os}^{\text{VI}}(\text{tpm})(\text{Cl})_2(\text{N})](\text{PF}_6)$ (**1**), $[\text{Os}^{\text{VI}}(\text{tpm})(\text{Cl})_2(^{15}\text{N})](\text{PF}_6)$ (**1***), $[\text{Os}^{\text{VI}}(\text{Tp})(\text{Cl})_2(\text{N})]$ (**2**), $[\text{Os}^{\text{VI}}(\text{Tp})(\text{Cl})_2(^{15}\text{N})]$ (**2***), $[\text{Os}^{\text{II}}(\text{tpm})(\text{Cl})_2(\text{NS})](\text{SCN})$ (**3a**), $[\text{Os}^{\text{II}}(\text{tpm})(\text{Cl})_2(^{15}\text{NS})](\text{SCN})$ (**3a***), $[\text{Os}^{\text{II}}(\text{tpm})(\text{Cl})_2(\text{NS})](\text{PF}_6)$ (**3b**), $[\text{Os}^{\text{II}}(\text{tpm})(\text{Cl})_2(^{15}\text{NS})](\text{PF}_6)$ (**3b***), $[\text{Os}^{\text{II}}(\text{tpm})(\text{Cl})_2(\text{NS})](\text{BF}_4)$ (**3c**), $[\text{Os}^{\text{II}}(\text{Tp})(\text{Cl})_2(\text{NS})]$ (**4**), $[\text{Os}^{\text{II}}(\text{Tp})(\text{Cl})_2(^{15}\text{NS})]$ (**4***), $[\text{Os}^{\text{IV}}(\text{tpm})(\text{Cl})_2(\text{NPPH}_3)]\text{PF}_6$ (**5**), $[\text{Os}^{\text{III}}(\text{tpm})(\text{Cl})_2(\text{NH}_3)]\text{PF}_6$ (**6**), $[\text{Os}^{\text{III}}(\text{tpm})(\text{Cl})_2(\text{NSO})\cdot 2\text{H}_2\text{O}]$ (**7**), $[\text{Os}^{\text{III}}(\text{tpm})(\text{Cl})_2(^{15}\text{NSO})\cdot 2\text{H}_2\text{O}]$ (**7***), and $[\text{Os}^{\text{II}}(\text{tpm})(\text{Cl})_2(\text{NO})]\text{BF}_4$ (**8**).

Abbreviations used in the text include the following: tpm, tris(1-pyrazolyl)-methane; Tp, hydrotris(1-pyrazolyl)borate anion; PPN^+ , bis-(triphenylphosphoranylidene) ammonium cation; TBAH, tetra-*n*-butylammonium hexafluorophosphate.

Materials. Osmium tetroxide (>99%) and potassium hydrotris(1-pyrazolyl)borate were purchased from Alfa-AESAR. Deuterated solvents and isotopically labeled reagents were purchased from Cambridge Isotope Laboratories. TBAH ($[\text{N}(n\text{-Bu})_4](\text{PF}_6)$), was recrystallized three times from boiling ethanol and dried under vacuum at 120 °C for 2 days. All other chemicals were of reagent grade and used without further purification.

Measurements. Electronic absorption spectra were acquired by using a Hewlett-Packard model 8452A diode array spectrophotometer. FT-IR spectra were recorded on a Mattson Galaxy Series 5000 instrument at 4 cm^{-1} resolution. Proton NMR spectra were recorded on Bruker AC200 (200 MHz) spectrometer. Elemental analyses were performed by Oneida Research Services, Inc. (Whitesboro, NY). Electrochemical measurements and electrolyses were conducted by using a PAR model 273 potentiostat and a three-compartment cell. For aqueous voltammetry, a 2.0 mm diameter glassy carbon disk working electrode (Bioanalytical Systems, West Lafayette, IN) was used. For nonaqueous measurements, the working electrode was a 1.0 mm platinum disk. The surface of the glassy carbon electrode was polished with diamond paste before use. All potentials are referenced to the saturated sodium chloride calomel electrode (SSCE, 0.24 V vs NHE) unless otherwise noted at room temperature and are uncorrected for junction potentials. In all cases, the auxiliary electrode was a coil of platinum wire. The solution in the working compartment was deoxygenated by nitrogen bubbling.

UV-visible measurements, with photodiode array detection for rapid kinetic experiments, were carried out on a Hi-Tech SF-61DX2 double-mixing, stopped-flow apparatus with fiber optic coupling to a Hamamatsu L2194-02 75 W xenon arc lamp. The system was interfaced with a personal computer by use of the KinetAsyst 2.0 software program. The temperature of solutions during kinetic studies was maintained by use of a Neslab RTE-110 circulating water bath.

The kinetics of the reaction between $[\text{Os}^{\text{II}}(\text{tpm})(\text{NS})(\text{Cl})_2](\text{PF}_6)$ and triphenylphosphine were studied by adding equal volumes of 5.22×10^{-3} M $[\text{Os}^{\text{II}}(\text{tpm})(\text{NS})(\text{Cl})_2](\text{PF}_6)$ and 0.050, 0.100, 0.150, 0.200, and 0.250 M PPh_3 . Absorbance changes were monitored at $\lambda_{\text{max}} = 636$ nm for $[\text{Os}^{\text{II}}(\text{tpm})(\text{NS})(\text{Cl})_2](\text{PF}_6)$. Under pseudo-first-order conditions with $[\text{PPh}_3] \gg [\text{Os}^{\text{II}}(\text{NS})^+]$, the reaction was first order in $[\text{Os}^{\text{II}}(\text{NS})^+]$. The pseudo first-order rate constant, k_{obs} , was determined by fitting the data to eq 1,

$$\ln \left[\frac{A_{\infty} - A_t}{A_0 - A_{\infty}} \right] = -k_{\text{obs}}t \quad (1)$$

with $k_{\text{obs}} = k[\text{PPh}_3]$. In eq 1, A_0 , A_t , and A_{∞} are the absorbances at time

0, t , and ∞ , respectively. A plot of k_{obs} vs $[\text{PPh}_3]$ was linear from 0.050 to 0.250 M. From the slope, $k(25^\circ\text{C}, \text{CH}_3\text{CN}) = 40 \pm 1 \text{ M}^{-1} \text{ s}^{-1}$.

Synthesis and Characterization. The following salts and compounds were prepared by literature procedures: $[\text{Os}^{\text{VI}}(\text{tpm})(\text{Cl})_2(\text{N})](\text{PF}_6)$ (**1**),⁸ $[\text{Os}^{\text{VI}}(\text{tpm})(\text{Cl})_2(^{15}\text{N})](\text{PF}_6)$ (**1***),⁸ $[\text{Os}^{\text{VI}}(\text{Tp})(\text{Cl})_2(\text{N})]$ (**2**),⁹ $[\text{Os}^{\text{VI}}(\text{Tp})(\text{Cl})_2(^{15}\text{N})]$ (**2***),⁹ tris(1-pyrazolyl)methane (tpm),¹⁰ and bis-(triphenylphosphoranylidene)ammonium azide (PPN) N_3 .^{6b}

$[\text{Os}^{\text{II}}(\text{tpm})(\text{Cl})_2(\text{NS})](\text{SCN})$ (3a**).** A quantity of $[\text{Os}^{\text{VI}}(\text{tpm})(\text{Cl})_2(\text{N})](\text{PF}_6)$ (**1**; 200 mg, 0.31 mmol) was dissolved in 10 mL of acetone. To this solution was added 20 mL of CS_2 , followed by a solution of $(\text{PPN})\text{N}_3$ (190 mg, 0.32 mmol) in 20 mL of acetone dropwise with stirring at room temperature over a 2 h period. A green solid formed as the reaction proceeded. It was filtered off, washed with acetone and Et_2O , and air-dried. Yield: 120 mg (65%). Anal. Calcd for $\text{C}_{11}\text{H}_{10}\text{Cl}_2\text{N}_8\text{OsS}_2$ (MW 579.94): C, 22.76; H, 1.74; N, 19.32. Found: C, 22.29; H, 1.95; N, 18.86. Infrared (cm^{-1} , KBr disk): $\nu(^{14}\text{N}=\text{S})$ 1320 (vs); $\nu(\text{tpm})$ 1508, 1445, 1409, and 1289; $\nu(\text{C}=\text{N})$ 2035.

$[\text{Os}^{\text{II}}(\text{tpm})(\text{Cl})_2(^{15}\text{NS})](\text{SCN})$ (3a***).** This salt was prepared by the same method by using $[\text{Os}^{\text{VI}}(\text{tpm})(\text{Cl})_2(^{15}\text{N})](\text{PF}_6)$ (**1***) as the starting material. Infrared (cm^{-1} , KBr disk): $\nu(^{15}\text{N}=\text{S})$ 1284.

$[\text{Os}^{\text{II}}(\text{tpm})(\text{Cl})_2(\text{NS})](\text{PF}_6)$ (3b**).** This salt was readily obtained from $[\text{Os}^{\text{II}}(\text{tpm})(\text{Cl})_2(\text{NS})](\text{SCN})$ (**3a**) by anion metathesis in water. For example, 50 mg (0.086 mmol) of **3a** was dissolved in 10 mL of H_2O containing excess NH_4PF_6 . The resulting reaction mixture was stirred for 5 h, during which time an olive green precipitate formed. It was filtered off, washed with H_2O , and recrystallized from $\text{CH}_3\text{CN}/\text{Et}_2\text{O}$. Yield: 40 mg (70%). Anal. Calcd for $\text{C}_{10}\text{H}_{10}\text{Cl}_2\text{N}_7\text{SO}_2\text{PF}_6$ (MW 666.93): C, 18.02; H, 1.51; N, 14.71. Found: C, 17.93; H, 1.65; N, 14.35. UV-vis (CH_3CN) λ_{max} , nm (ϵ , $\text{M}^{-1} \text{cm}^{-1}$): 636 (160), 434 (210), 300 (1.61×10^4), 274 (1.95×10^4), 220 (3.10×10^4). Infrared (cm^{-1} , KBr disk): $\nu(^{14}\text{N}=\text{S})$ 1317 (vs); $\nu(\text{tpm})$ 1508, 1444, 1409, and 1284; $\nu(\text{P}-\text{F})$ 831.

$[\text{Os}^{\text{II}}(\text{tpm})(\text{Cl})_2(^{15}\text{NS})](\text{PF}_6)$ (3b***).** This salt was prepared by the same method as for **3b** except that $[\text{Os}^{\text{II}}(\text{tpm})(\text{Cl})_2(^{15}\text{NS})](\text{SCN})$ (**3a***) was used as the starting material. Infrared (cm^{-1} , KBr disk): $\nu(^{15}\text{N}=\text{S})$ 1284 (vs).

$[\text{Os}^{\text{II}}(\text{tpm})(\text{Cl})_2(\text{NS})](\text{BF}_4)$ (3c**).** This salt was prepared by the same method as for $[\text{Os}^{\text{II}}(\text{tpm})(\text{Cl})_2(\text{NS})](\text{PF}_6)$ (**3b**) except that the reaction was carried out in CH_3OH with addition of KBF_4 . Yield (65%). Infrared (cm^{-1} , KBr disk): $\nu(^{14}\text{N}=\text{S})$ 1316 (vs); $\nu(\text{tpm})$ 1508, 1445, 1410, and 1285; $\nu(\text{B}-\text{F})$ 1060 (vs). ^1H NMR (200 MHz, CD_3CN): δ/ppm 6.51 (t, 1H), 6.82 (t, 2H), 7.88 (d, 1H), 8.09 (d, 1H), 8.26 (d, 2H), 8.45 (d, 2H), 9.21 (s, 1H).

$[\text{Os}^{\text{II}}(\text{Tp})(\text{Cl})_2(\text{NS})]$ (4**).** A quantity of $[\text{Os}^{\text{VI}}(\text{Tp})(\text{Cl})_2(\text{N})]$ (**2**) (200 mg, 0.40 mmol) was dissolved in 10 mL of acetone. To this solution was added 20 mL of CS_2 , followed by a solution of $(\text{PPN})\text{N}_3$ (240 mg, 0.41 mmol) in 20 mL acetone which was added dropwise while stirring at room temperature for 3 h. During the addition of the azide, the color of the reaction mixture changed from orange to dark green, and a green solid was formed. This solid was filtered off, washed with acetone and then Et_2O , and air-dried. Yield: 140 mg (65%). Anal. Calcd for $\text{C}_9\text{H}_{10}\text{Cl}_2\text{N}_7\text{OsBS}$ (MW 520.98): C, 20.73; H, 1.93; N, 18.81. Found: C, 19.64; H, 1.72; N, 17.28. UV-vis (CH_3CN) λ_{max} , nm (ϵ , $\text{M}^{-1} \text{cm}^{-1}$): 646 (120), 436 (150), 288 (2.15×10^4), 252 (1.53×10^4), 222 (3.00×10^4). Infrared (cm^{-1} , KBr disks): $\nu(^{14}\text{N}=\text{S})$ 1284 (vs); $\nu(\text{B}-\text{H})$ 2528 (vs); $\nu(\text{Tp})$ 1502, 1407, and 1320.

$[\text{Os}^{\text{II}}(\text{Tp})(\text{Cl})_2(^{15}\text{NS})]$ (4***).** This compound was prepared by the same method by using $[\text{Os}^{\text{VI}}(\text{Tp})(\text{Cl})_2(^{15}\text{N})]$ (**2***) as the starting material. Infrared (cm^{-1} , KBr disks): $\nu(^{15}\text{N}=\text{S})$ 1247 (vs).

$[\text{Os}^{\text{VI}}(\text{tpm})(\text{Cl})_2(\text{NPPH}_3)](\text{PF}_6)$ (5**).** A quantity of $[\text{Os}^{\text{II}}(\text{tpm})(\text{Cl})_2(\text{NS})](\text{PF}_6)$ (**1b**) (120 mg, 0.18 mmol) was dissolved in 20 mL of CH_3CN . PPh_3 (95 mg, 0.36 mmol) was added as a solid in one portion

(8) Demadis, K. D.; El-Samanody, E.-S.; Coia, G. M.; Meyer, T. J. *J. Am. Chem. Soc.* **1998**, *121*, 535.

(9) (a) Crevier, T. J.; Mayer, J. M. *J. Am. Chem. Soc.* **1998**, *120*, 5595. (b) Crevier, T. J.; Mayer, J. M. *Angew. Chem., Int. Ed.* **1998**, *37*, 1891. (c) Crevier, T. J.; Lovell, S.; Mayer, J. M.; Rheingold, A. L.; Guzei, I. A. *J. Am. Chem. Soc.* **1998**, *120*, 6607.

(10) (a) Huchel, W.; Bretschneider, H. *Ber. Chem.* **1937**, *9*, 2024. (b) Byers, P. K.; Canty, A. J.; Honeyman, R. T. *J. Organomet. Chem.* **1990**, *385*, 421.

while stirring, causing an immediate change in color from green to brown. The reaction mixture was stirred for 30 min. Addition of 150 mL of anhydrous Et₂O caused precipitation of a brown precipitate, which was filtered off, washed with Et₂O, and air-dried. Yield: 135 mg (83%). Anal. Calcd for C₂₈H₂₅Cl₂N₇O₈P₂F₆ (MW 897.05): C, 37.51; H, 2.81; N, 10.94. Found: C, 37.73, H, 2.82, N, 11.22. UV-vis (CH₃-CN) λ_{\max} , nm (ϵ , M⁻¹ cm⁻¹): 516 (115), 390 (4.43 × 10³), 302 (7.83 × 10³), 228 (1.63 × 10⁴), 216 (1.86 × 10⁴). Infrared (cm⁻¹, KBr disks): ν (tpm) 1436, 1405, and 1276; ν (N=P) 1108 (vs); ν (P-F) 833 (vs). The elemental analyses and spectroscopic properties of this material compare well with an authentic sample of [Os^{IV}(tpm)(Cl)₂-(NPPH₃)](PF₆) prepared by an alternate synthetic route.¹¹

[Os^{III}(tpm)(Cl)₂(NH₃)](PF₆) (6). A quantity of [Os^{II}(tpm)(Cl)₂(NS)]-(PF₆) (**3b**) (200 mg, 0.3 mmol) was dissolved in 50 mL of 3 M HCl. Several pieces of amalgamated zinc were added, and the mixture was stirred vigorously for 30 min. The color of the reaction mixture turned from dark green to pale yellow with the smell of H₂S gas. Excess zinc was removed by filtration, and solid NH₄PF₆ in excess was added to the filtrate. Evaporation of the mixture to 10 mL by rotary evaporation and cooling at 5 °C for 1 h caused precipitation of a tan compound. It was filtered off and recrystallized from CH₃CN/Et₂O. Yield: 115 mg (60%). UV-vis (CH₃CN): λ_{\max} , nm (ϵ , M⁻¹ cm⁻¹) 320 (6.60 × 10³), 290 (9.10 × 10³), 204 (1.26 × 10⁴). Infrared (cm⁻¹, KBr disks): ν (N-H) 3338, 3256; ν (tpm) 1512, 1445, 1409, 1279; ν (P-F) 850. The spectroscopic and electrochemical properties of this material compare well with an authentic sample of [Os^{III}(tpm)(Cl)₂(NH₃)](PF₆) prepared by an alternate synthetic route.¹²

[Os^{III}(tpm)(Cl)₂(NSO)·2H₂O (7). A quantity of [Os^{II}(tpm)(Cl)₂(NS)]-(PF₆) (**3b**; 180 mg, 0.27 mmol) was dissolved in 100 mL of CH₃CN. To that solution was added a 10-fold excess of trimethylamine *N*-oxide dihydrate as solid. The reaction mixture was stirred for 30 min. During this time, the color of the reaction mixture turned from green to brown with formation of a fine gray precipitate. It was isolated by filtration and thoroughly washed with CH₃CN and Et₂O. Yield: 130 mg (84%). Anal. Calcd for C₁₀H₁₀Cl₂N₇O₈SO·2H₂O (MW 573.98): C, 20.91; H, 2.46; N, 17.08. Found: C, 20.79; H, 2.30; N, 16.84. UV-vis (DMSO) λ_{\max} , nm (ϵ , M⁻¹ cm⁻¹): 556 (35), 468 (130), 350 (3.10 × 10³), 290 (7.54 × 10³). Infrared (cm⁻¹, KBr disk): $\nu_{\text{as}}(\text{NSO})$ 1197 (vs), $\nu_{\text{s}}(\text{NSO})$ 1024 (vs), $\delta(\text{NSO})$ 538 (w); ν (tpm) 1508 (vs), 1438 (vs), 1408 (vs), 1270 (vs).

[Os^{III}(tpm)(Cl)₂(¹⁵NSO)·2H₂O (7*). This compound was prepared by the same method by using [Os^{II}(tpm)(Cl)₂(¹⁵NS)]PF₆ as the starting material. Infrared (cm⁻¹, KBr disk): $\nu_{\text{as}}(\text{¹⁵NSO})$ 1182 (vs), $\nu_{\text{s}}(\text{¹⁵NSO})$ 1010 (vs), $\delta(\text{¹⁵NSO})$ 524 (w).

Reaction of [Os^{II}(tpm)(Cl)₂(NS)](BF₄) (3c) with NOBF₄. A quantity of [Os^{II}(tpm)(Cl)₂(NS)](BF₄) (150 mg, 0.24 mmol) was dissolved in 10 mL of CH₃CN. NOBF₄ (170 mg, 1.45 mmol) was added as a solid while stirring. The reaction mixture was stirred for 30 min during which time the color turned from green to dark orange. The reaction mixture was taken to dryness by rotary evaporation to give a dark orange oily material. It was treated with 60 mL of CH₂Cl₂ and filtered, leaving an unidentified orange oily material on the frit. The solution was reduced in volume to 5 mL by rotary evaporation. Addition of 100 mL of anhydrous ether caused precipitation of an orange product. It was collected by filtration, washed with Et₂O, and air-dried. The product was shown to be a mixture of [Os^{II}(tpm)(Cl)₂(NO)](BF₄) and [Os^V(tpm)(Cl)₂(N)](BF₄) in ~1:4 ratio as shown by electrochemical measurements (see below). Anal. Calcd for C₁₀H₁₀Cl₂N₇O_{0.2}OsBF₄ (MW 580.20) (for a 1:4 mixture): C, 20.73 H, 1.74; N, 16.97. Found: C, 20.40; H, 1.68; N, 17.06. Infrared (cm⁻¹, KBr disk): $\nu(\text{NO})$ 1870 (vs); ν (tpm) 1513 (vs), 1446 (vs), 1408 (vs), 1288 (vs), 1261 (vs); $\nu(\text{B-F})$ 1056 (vs).

When this reaction was repeated with Os¹⁵NS as starting material, the same product mixture was obtained. Infrared (cm⁻¹, KBr disk): $\nu(\text{NO})$ 1872 (vs).

X-ray Structural Determinations. Data Collection, Solution, and Refinement of the Structures. Single crystals of [Os^{II}(tpm)(Cl)₂(NS)]-

Table 1. Summary of Crystal Data, Intensity Collection and Structure Refinements Parameters for [Os^{II}(tpm)(Cl)₂(NS)](BF₄) (**3c**), and Os^{II}(Tp)(Cl)₂(NS) (**4**)

	3c	4
empirical formula	C ₁₀ H ₁₀ Cl ₂ N ₇ O ₈ SBF ₄	C ₉ H ₁₀ Cl _{2.11} N _{6.89} O ₈ S _{0.89} B
mol wt	608.20	518.99
<i>a</i> (Å)	10.4435(15)	7.7429(5)
<i>b</i> (Å)	11.9036(17)	12.8192(9)
<i>c</i> (Å)	14.1321(20)	8.4385(6)
α (deg)	90	90
β (deg)	90	114.416(1)
γ (deg)	90	90
<i>V</i> (Å ³)	1756.8(4)	762.68(9)
<i>Z</i>	4	2
cryst syst	orthorhombic	monoclinic
space group	<i>Pmnb</i>	<i>P21</i>
cryst size (mm)	0.30 × 0.15 × 0.10	0.30 × 0.10 × 0.05
<i>d</i> _{calcd} (g/cm ³)	2.299	2.260
diffractometer	Siemens CCD Smart	Siemens CCD Smart
radiation	Mo K α (λ = 0.710 73 Å)	Mo K α (λ = 0.710 73 Å)
collection temp	-100 °C	-100 °C
abs coefficient μ , cm ⁻¹	7.73	8.85
<i>F</i> (000)	1142.95	485.97
$2\theta_{\max}$ (dgc)	50	60
no. of total reflections	15 707	9405
no. of unique reflections	1649	4172
no. of refined reflections	1028	1852
merging <i>R</i> value	0.112	0.027
no. of parameters	136	193
<i>R</i> (%) ^a	3.2	3.2
<i>R</i> _w (%) ^b	3.8	3.3
goodness of fit ^c	0.61	1.81
deepest hole (e/Å ³)	-0.970	-1.910
highest peak (e/Å ³)	2.040	3.8

$$^a R = \sum(|F_o - F_c|) / \sum|F_o|. \quad ^b R_w = [\sum(w|F_o - F_c|)^2 / \sum w(F_o)^2]^{1/2}. \quad ^c G = [\sum w(F_o - F_c)^2 / (\text{no. of reflections} - \text{no. of parameters})]^{1/2}.$$

(BF₄) (**3c**) were obtained by layering a CH₂Cl₂ solution with Et₂O. Single crystals of Os^{II}(Tp)(Cl)₂(NS) (**4**) were obtained by slow diffusion of Et₂O into a DMF solution. Crystal data, intensity collection information, and structure refinement parameters for the structures are provided in Table 1. The structures were solved by direct methods. The remaining non-hydrogen atoms were located in subsequent difference Fourier maps. Empirical absorption corrections were applied with SADABS. The ORTEP plotting program was used to computer generate the structures shown in Figures 2 and 3.¹³ Hydrogen atoms were included in calculated positions with thermal parameters derived from the atom to which they were bonded. All computations were performed by using the NRCVAX suite of programs.¹⁴ Atomic scattering factors were taken from a standard source¹⁵ and corrected for anomalous dispersion. The final positional parameters along with their standard deviations as estimates from the inverse matrix, tables of hydrogen atom parameters, anisotropic thermal parameters, and observed/calculated structure amplitudes for **3c** and **4** are available as Supporting Information. Selected bond lengths and angles of **3c** and **4** are given in Tables 2 and 3.

Results

Synthesis and Characterization. The preparation and probable mechanism of formation of the thionitrosyls based on the reaction between an adduct between CS₂ and N₃⁻ with the Os^V

- (11) El-Samanody, E.-S. Demadis, K. D.; Meyer, T. J.; White, P. S. Work in progress.
 (12) El-Samanody, E.-S. Demadis, K. D.; Meyer, T. J.; White, P. S. Manuscript in preparation.

- (13) Johnson, C. K. *ORTEP: A Fortran thermal ellipsoid plot program*; Technical Report ORNL-5138; Oak Ridge National Laboratory: Oak Ridge, TN, 1976.
 (14) Gabe, E. J.; Le Page, Y.; Charland, J.-P.; Lee, F. L.; White, P. S. *J. Appl. Crystallogr.* **1989**, *22*, 384.
 (15) *International Tables for X-ray Crystallography*; Kynoch Press: Birmingham, UK, 1974; Vol. IV.

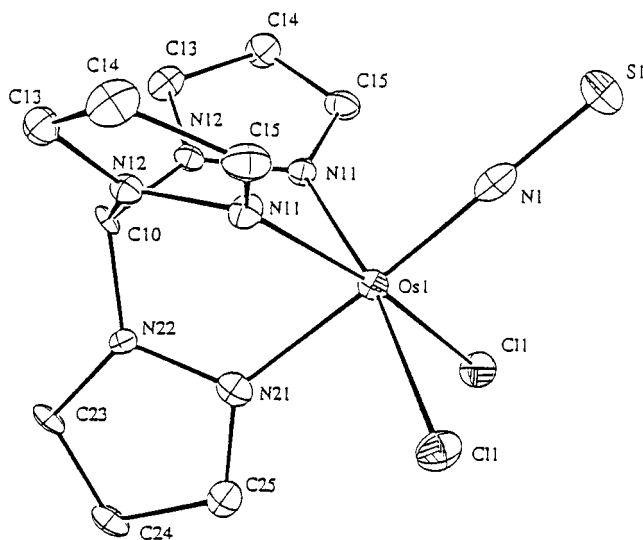


Figure 2. ORTEP diagram (30% probability ellipsoids) for the $[\text{Os}^{\text{II}}(\text{tpm})(\text{Cl})_2(\text{NS})]^+$ cation in **3c**.

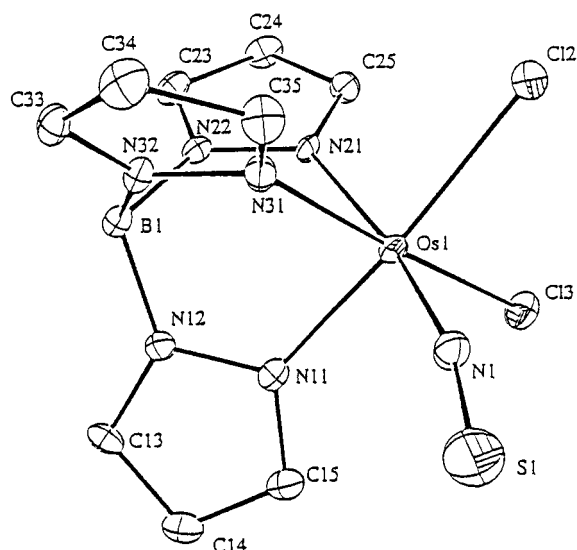
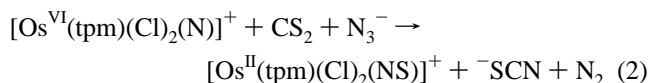


Figure 3. ORTEP diagram (30% probability ellipsoids) for $\text{Os}^{\text{II}}(\text{Tp})(\text{Cl})_2(\text{NS})$ (**4**) as a cocrystal with 11% $\text{Os}^{\text{IV}}(\text{Tp})(\text{Cl})_3$.

nitrido complexes was discussed earlier.⁶ The net reaction for the tpm complex is



Molecular Structures. ORTEP diagrams with labeling schemes for the cation in $[\text{Os}^{\text{II}}(\text{tpm})(\text{Cl})_2(\text{NS})](\text{BF}_4)$ (**3c**) and $\text{Os}^{\text{II}}(\text{Tp})(\text{Cl})_2(\text{NS})$ (**4**) are shown in Figures 2 and 3 respectively. The crystal of **3c** has well-separated $[\text{Os}^{\text{II}}(\text{tpm})(\text{Cl})_2(\text{NS})]^+$ cations and BF_4^- anions. **3c** resides on a crystallographically imposed mirror plane that includes one pyrazolate ring (trans to the NS^+), the Os center, and the NS^+ ligand. The Os–N(S) and N–S bond lengths are 1.780(14) Å and 1.489(15) Å, respectively. $\angle\text{Os}–\text{N}–\text{S}$ is virtually linear at 179.3(9)°. The Os–Cl bond length is 2.355(3) Å, and Os–N(ring) bond lengths range from 2.083(8) to 2.086(13) Å. Bond lengths in the pyrazolate rings are unremarkable and are consistent with those found in several literature structures.^{11,12,16}

(16) Llobet, A.; Hodgson, D. J.; Meyer, T. J. *Inorg Chem.* **1990**, *29*, 3760.

Table 2. Selected Bond Distances (Å) and Bond Angles (deg) for $[\text{Os}^{\text{II}}(\text{tpm})(\text{Cl})_2(\text{NS})](\text{BF}_4)$ (**3c**); Labeling as in Figure 2^a

Bond Distances			
Os(1)–Cl(1)	2.355(3)	Os(1)–N(11)a	2.083(8)
Os(1)–Cl(1)a	2.355(3)	Os(1)–N(21)	2.086(13)
Os(1)–N(1)	1.780(14)	S(1)–N(1)	1.489(15)
Os(1)–N(11)	2.083(8)		

Bond Angles			
Cl(1)–Os(1)–Cl(1)a	89.57(10)	Cl(1)a–Os(1)–N(21)	87.7(3)
Cl(1)–Os(1)–N(1)	95.5(3)	N(1)–Os(1)–N(11)	93.3(4)
Cl(1)–Os(1)–N(11)	91.92(24)	N(1)–Os(1)–N(11)a	93.3(4)
Cl(1)–Os(1)–N(11)a	170.92(25)	N(1)–Os(1)–N(21)	175.5(5)
Cl(1)–Os(1)–N(21)	87.7(3)	N(11)–Os(1)–N(11)a	85.2(3)
Cl(1)a–Os(1)–N(1)	95.5(3)	N(11)–Os(1)–N(21)	83.4(4)
Cl(1)a–Os(1)–N(11)	170.92(25)	N(11)a–Os(1)–N(21)	83.4(4)
Cl(1)a–Os(1)–N(11)a	91.92(24)	Os(1)–N(1)–S(1)	179.3(9)

^a The bond distances and angles labeled a arise from the existence of a mirror plane between the two chlorides and two pyrazolyl rings.

Table 3. Selected Bond Distances (Å) and Bond Angles (deg) for $\text{Os}^{\text{II}}(\text{Tp})(\text{Cl})_2(\text{NS})$ (**4**); Labeling as in Figure 3

Bond Distances			
Os(1)–Cl(1)	2.325(18)	Os(1)–N(11)	2.086(5)
Os(1)–Cl(2)	2.3541(16)	Os(1)–N(21)	2.125(5)
Os(1)–Cl(3)	2.3457(18)	Os(1)–N(31)	2.066(6)
Os(1)–N(1)	1.800(8)	S(1)–N(1)	1.493(8)

Bond Angles			
Cl(1)–Os(1)–Cl(2)	95.6(4)	Cl(3)–Os(1)–N(31)	174.68(16)
Cl(1)–Os(1)–Cl(3)	89.3(4)	N(1)–Os(1)–N(11)	89.2(3)
Cl(1)–Os(1)–N(1)	6.5(5)	N(1)–Os(1)–N(21)	170.6(3)
Cl(1)–Os(1)–N(11)	91.1(4)	N(1)–Os(1)–N(31)	89.7(3)
Cl(1)–Os(1)–N(21)	175.0(4)	N(11)–Os(1)–N(21)	83.87(20)
Cl(1)–Os(1)–N(31)	96.0(5)	N(11)–Os(1)–N(31)	88.85(20)
Cl(2)–Os(1)–Cl(3)	89.44(6)	N(21)–Os(1)–N(31)	83.76(21)
Cl(2)–Os(1)–N(1)	97.53(23)	Os(1)–Cl(1)–S(1)	142.3(13)
Cl(2)–Os(1)–N(11)	173.23(15)	Os(1)–Cl(1)–N(1)	20.8(16)
Cl(2)–Os(1)–N(21)	89.35(14)	S(1)–Cl(1)–N(1)	122.1(25)
Cl(2)–Os(1)–N(31)	90.34(15)	Cl(1)–S(1)–N(1)	19.0(9)
Cl(3)–Os(1)–N(1)	95.55(25)	Os(1)–N(1)–Cl(1)	152.7(20)
Cl(3)–Os(1)–N(11)	90.75(15)	Os(1)–N(1)–S(1)	166.9(5)
Cl(3)–Os(1)–N(21)	90.93(15)	Cl(1)–N(1)–S(1)	38.9(18)

The crystal of neutral **4** includes two molecules: $\text{Os}^{\text{II}}(\text{tpm})(\text{Cl})_2(\text{NS})$ (89%) and $\text{Os}^{\text{IV}}(\text{Tp})(\text{Cl})_3$ (11%). In the initial stages of refinement, $\angle\text{Os}–\text{N}–\text{S}$ appeared to be abnormally acute. This angle and the large thermal ellipsoid of the thionitrosyl N indicated cocrystallization with another very similar molecule. It was brought to our attention¹⁷ that in the synthesis of $\text{Os}^{\text{VI}}(\text{Tp})(\text{Cl})_2(\text{N})$ (**2**), $\text{Os}^{\text{IV}}(\text{Tp})(\text{Cl})_3$ often appears as a contaminant. Reevaluation of the collected data and re-refinement of the structure with the aforementioned composition yielded satisfactory and reliable metric features. $\angle\text{Os}–\text{N}–\text{S}$ is slightly bent at 166.9(5)°. The Os–N(S) and N–S bond lengths are 1.800(8) and 1.493(8) Å, respectively. The Os–Cl bond lengths are 2.3541(16) and 2.3457(18) Å, and Os–N(ring) bond lengths range from 2.066(6) to 2.125(5) Å. Note that the longest Os–N(ring) bond length is found trans to the thionitrosyl ligand. The discrepancy in Os–N(ring) bond lengths in **4** is in contrast to the analogous bond lengths in **3c**, which are virtually identical. Bond lengths in the pyrazolate rings are unremarkable and are consistent with those found in several Tp literature examples.^{9,18}

(17) Crevier, T. J.; Mayer, J. M. Personal communication.

(18) (a) Koch, J. L.; Shapely, P. A. *Organometallics* **1997**, *16*, 4071. (b) Schrock, R. R.; Lapointe, A. M. *Organometallics* **1993**, *12*, 3379. (c) Lapointe, A. M.; Schrock, R. R.; Davies, W. M. *J. Am. Chem. Soc.* **1995**, *117*, 4802. (d) Gunnoe, T.; Sabat, M.; Harman, W. D. *J. Am. Chem. Soc.* **1998**, *120*, 8747.

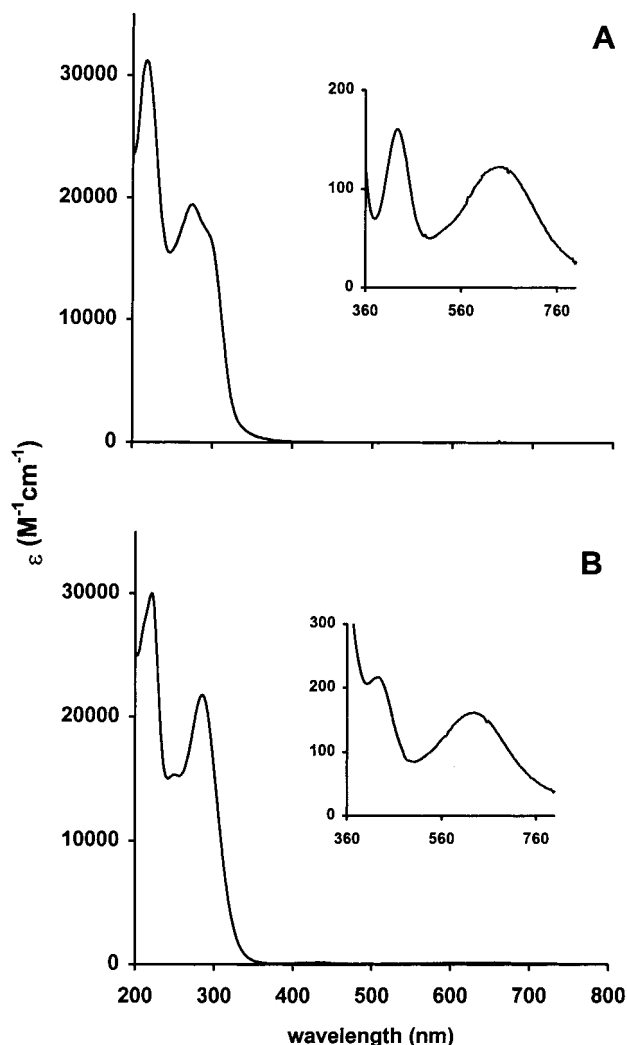


Figure 4. UV-visible spectra of $[\text{Os}^{\text{II}}(\text{tpm})(\text{Cl})_2(\text{NS})](\text{PF}_6)$ (**3b**) (A) and $\text{Os}^{\text{II}}(\text{Tp})(\text{Cl})_2(\text{NS})$ (**4**) (B) in CH_3CN . Expanded views of the spectra from 360 to 760 nm are shown as inserts.

Spectroscopy. UV-vis data for the new products are summarized in the Experimental Section, and spectra of **3b** and **4** are shown in Figure 4. Bands of low absorptivity appear in the visible region at 636 and 432 nm ($\epsilon = 160$ and $210 \text{ M}^{-1} \text{ cm}^{-1}$, respectively) for **3b** and at 646 and 434 nm ($\epsilon = 160$ and $210 \text{ M}^{-1} \text{ cm}^{-1}$) for **4**, as well as typical $\pi \rightarrow \pi^*$ (tpm or Tp) bands in the UV.⁸

In the IR spectra of the Os^{14}NS and Os^{15}NS forms of $[\text{Os}^{\text{II}}(\text{tpm})(\text{Cl})_2(\text{NS})](\text{PF}_6)$ (**3b**) and $\text{Os}^{\text{II}}(\text{Tp})(\text{Cl})_2(\text{NS})$ (**4**) in the region $1350\text{--}1200 \text{ cm}^{-1}$ (Figure 1 in the Supporting Information). $\nu(\text{N}=\text{S})$ appears as a sharp band at 1317 cm^{-1} for **3b**. It is shifted to 1287 in the ^{15}N -labeled analogue. For **4**, $\nu(\text{N}=\text{S})$ appears as a split band at 1288 and 1284 cm^{-1} and is shifted to 1253 and 1249 cm^{-1} in **4***. The value for **4** compares well with the value for $\text{Os}^{\text{II}}(\text{Tp})(\text{Cl})_2(\text{NS})$ prepared by another synthetic route.^{9c}

Low-intensity bands also appear in the region $540\text{--}420 \text{ cm}^{-1}$ (Figure 2 in the Supporting Information), which are shifted by $\sim 15 \text{ cm}^{-1}$ in ^{15}N -labeled complexes. More specifically, for **3b** bands appear at 495 and 482 cm^{-1} , which are shifted to 482 and 468 cm^{-1} in **3b***. For **4**, these bands appear at 512 , 484 , and 451 cm^{-1} and are shifted to 499 , 470 , and 433 cm^{-1} in **4***.

A characteristic band appears at 2035 cm^{-1} for the SCN^- counterion in **3a**, at 2050 cm^{-1} in $(\text{PPN})(\text{SCN})$, obtained as a

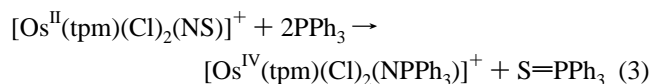
byproduct of the reaction between **2** and CS_2 with added $(\text{PPN})\text{N}_3$. $\nu(\text{B-H})$ in **4** appears at 2505 cm^{-1} .

Transition metal complexes containing the thiazato ligand (NSO^-) have characteristic NSO bands in the regions $1260\text{--}1118$, $1090\text{--}1010$, and $630\text{--}515 \text{ cm}^{-1}$, which are assigned to $\nu_{\text{as}}(\text{NSO})$, $\nu_{\text{s}}(\text{NSO})$, and $\delta(\text{NSO})$, respectively.^{6e,19} In the IR spectrum of $\text{Os}^{\text{III}}(\text{tpm})(\text{Cl})_2(\text{NSO})$ (**7**), these bands appear at 1197 , 1024 , and 534 cm^{-1} and are shifted in ^{15}N -labeled **7*** to 1182 , 1010 , and 524 cm^{-1} .

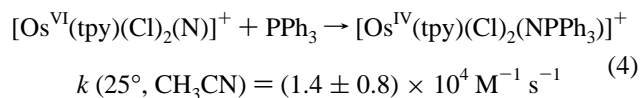
The $\text{Os}^{\text{II}}\text{NS}$ complexes are diamagnetic. From the ^1H NMR spectrum of **3c** in CD_3CN , a series of resonances appears characteristic of the tpm ligand.^{16,20}

Reactivity. A series of NS-based reactions were investigated for $[\text{Os}^{\text{II}}(\text{tpm})(\text{Cl})_2(\text{NS})]^+$.

Reaction with PPh_3 . A rapid reaction occurs upon mixing excess PPh_3 and **1b** in CH_3CN . The products of the reaction were $[\text{Os}^{\text{IV}}(\text{tpm})(\text{Cl})_2(\text{NPPH}_3)](\text{PF}_6)$ and $\text{S}=\text{PPh}_3$.



Triphenylphosphine sulfide ($\text{S}=\text{PPh}_3$) was extracted with Et_2O , and after evaporation of the solvent, was isolated as a powder. An IR spectrum of this material in KBr showed characteristic bands for $\text{S}=\text{PPh}_3$ at 1306 , 1101 , 714 , and 517 cm^{-1} , which match to those of an authentic sample (Aldrich). $[\text{Os}^{\text{IV}}(\text{tpm})(\text{Cl})_2(\text{NPPH}_3)](\text{PF}_6)$ was identified by elemental analysis and by its UV-visible spectrum with $\lambda_{\text{max}} = 390 \text{ nm}$ ($\epsilon = 4400 \text{ M}^{-1} \text{ cm}^{-1}$). With one equivalent of PPh_3 , the reaction products were $0.5 \text{ S}=\text{PPh}_3$, $[\text{Os}^{\text{IV}}(\text{tpm})(\text{Cl})_2(\text{NPPH}_3)]^+$, and unreacted thionitrosyl as shown by UV-visible measurements. Formation of $[\text{Os}^{\text{IV}}(\text{tpm})(\text{Cl})_2(\text{NPPH}_3)]^+$ as the final product is expected if the nitrido complex $[\text{Os}^{\text{VI}}(\text{tpm})(\text{Cl})_2(\text{N})]^+$ is an intermediate. The reaction between Os^{VI} nitrido and PPh_3 is known to be rapid.²¹



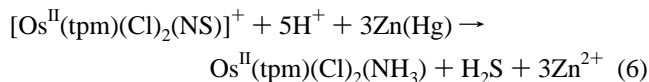
Based on the results of the kinetics study, with PPh_3 in excess, the rate law is

$$\frac{-d[\text{Os}(\text{NS})^+]}{dt} = k[\text{Os}(\text{NS})^+][\text{PPh}_3] = k_{\text{obs}}[\text{Os}(\text{NS})^+] \quad (5)$$

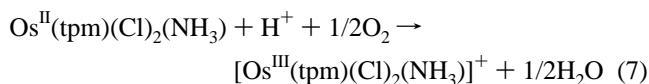
From the slope of a plot of k_{obs} vs $[\text{PPh}_3]$, $k(25^\circ \text{C}, \text{CH}_3\text{CN}) = 40 \pm 1 \text{ M}^{-1} \text{ s}^{-1}$.

Reduction by Amalgamated Zn. In 3 M HCl , over $\text{Zn}(\text{Hg})$, in the presence of air, **1b** undergoes a reaction over a period of $\sim 1/2$ h. The product was identified as $[\text{Os}^{\text{III}}(\text{tpm})(\text{Cl})_2(\text{NH}_3)](\text{PF}_6)$ by the appearance of its characteristic $\text{Os}^{\text{III}}/\text{Os}^{\text{II}}$ and $\text{Os}^{\text{IV}}/\text{Os}^{\text{III}}$ couples at $E_{1/2} = -0.36$ and $+0.95 \text{ V}$ vs SSCE in 3 M HCl as measured by cyclic voltammetry.¹² In the net reaction, $\text{Os}^{\text{II}}\text{NS}^+$ is reduced to $\text{Os}^{\text{II}}\text{--NH}_3$ and H_2S .

- (19) (a) Bohle, D. S.; Hung, C.-H.; Powell, A. K.; Smith, B. D.; Wocadlo, S. *Inorg. Chem.* **1997**, *36*, 1992. (b) Tiwari, R. D.; Pandey, K. K.; Agarwala, U. C. *Inorg. Chem.* **1982**, *21*, 845. (c) Pandey, K. K. *Inorg. Chim. Acta* **1991**, *182*, 171. (d) Pandey, K. K.; Nehete, D. T.; Tewari, S. K.; Rewari, S.; Bhardwaj, R. *Polyhedron* **1988**, *7*, 709.
 (20) Llobet, A.; Doppelt, P.; Meyer, T. J. *Inorg. Chem.* **1988**, *27*, 514.
 (21) (a) Demadis, K. D.; Bakir, M.; Kleszczewski, B. G.; Williams, D. S.; White, P. S.; Meyer, T. J. *Inorg. Chim. Acta* **1998**, *270*, 511. (b) Bakir, M.; White, P. S.; Doveloglou, A.; Meyer, T. J. *Inorg. Chem.* **1991**, *30*, 2835.



and H_2S detected by its characteristic odor. In the presence of air, the ammine complex undergoes O_2 oxidation to $\text{Os}^{\text{III}}\text{-NH}_3^+$.

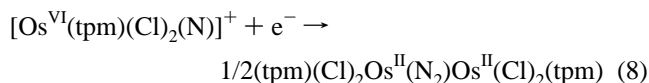


Reaction with $\text{O}=\text{NMe}_3$. Reaction occurs between $[\text{Os}^{\text{II}}(\text{tpm})(\text{Cl})_2(\text{NS})](\text{PF}_6)$ (**1b**) and trimethylamine *N*-oxide in CH_3CN upon mixing, with precipitation of a gray solid from the solution. The solid was characterized as $\text{Os}^{\text{III}}(\text{tpm})(\text{Cl})_2(\text{NSO})$ by elemental analyses and IR (Experimental).

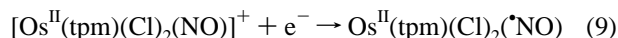
Reaction with NO^+ . When **1c** was allowed to react with excess NOBF_4 in CH_3CN , a color change occurs from green to deep orange over a period of 5 min. The products were identified as a mixture of $[\text{Os}^{\text{II}}(\text{tpm})(\text{Cl})_2(\text{NO})](\text{BF}_4)$ and $[\text{Os}^{\text{VI}}(\text{tpm})(\text{Cl})_2(\text{N})](\text{BF}_4)$ as follows.

(1) In the IR spectrum, an intense band for $\nu(\text{NO})$ appears at 1870 cm^{-1} . For comparison, $\nu(\text{NO})$ in *trans*- $[\text{Os}^{\text{II}}(\text{tpy})(\text{Cl})_2(\text{NO})]^+$ appears at 1868 cm^{-1} .²² When the reaction was repeated with $\text{Os-}^{15}\text{N}^+$, there was no IR shift in $\nu(\text{NO})$ in the $[\text{Os-NO}]^+$ product.

(2) In cyclic voltammograms of the product mixture in CH_3CN in 0.1 M TABH (Figure 3 in the Supporting Information), characteristic waves for the $\text{Os}^{\text{III}}(\text{N}_2)\text{Os}^{\text{III}}/\text{Os}^{\text{III}}(\text{N}_2)\text{Os}^{\text{II}}$ and $\text{Os}^{\text{III}}(\text{N}_2)\text{Os}^{\text{II}}/\text{Os}^{\text{II}}(\text{N}_2)\text{Os}^{\text{II}}$ couples of $(\text{tpm})(\text{Cl})_2\text{Os}^{\text{II}}(\text{N}_2)\text{Os}^{\text{II}}(\text{Cl})_2(\text{tpm})$ appear at $E_{1/2} = +0.77$ and $+0.12$ V. The $\mu\text{-N}_2$ complex is known to be formed by electrochemical reduction of $[\text{Os}^{\text{VI}}(\text{tpm})(\text{Cl})_2(\text{N})]^+$ at $E_{\text{pc}} = -0.47$ V in CH_3CN .^{6,8}



(3) A new wave also appears at $E_{1/2} = -0.10$ V, which based on related nitrosyl complexes, can be assigned as an NO-based reduction,²³



From the relative peak currents, the relative amounts of $[\text{Os}^{\text{II}}(\text{tpm})(\text{Cl})_2(\text{NO})]^+$ and $(\text{tpm})(\text{Cl})_2\text{Os}^{\text{II}}(\text{N}_2)\text{Os}^{\text{II}}(\text{Cl})_2(\text{tpm})$ are $\sim 1:2$, and the initial $[\text{Os}^{\text{II}}(\text{tpm})(\text{Cl})_2(\text{NO})]^+$ to $[\text{Os}^{\text{VI}}(\text{tpm})(\text{Cl})_2(\text{N})]^+$ ratio is $\sim 1:4$.

Electrochemistry. There is no evidence for oxidation of **3b** or **4** to the solvent limit of ~ 2 V. Reductions of $[\text{Os}^{\text{II}}(\text{tpm})(\text{Cl})_2(\text{NS})]^+$ (**3b**) and $\text{Os}^{\text{II}}(\text{Tp})(\text{Cl})_2(\text{NS})$ (**4**) in CH_3CN are chemically irreversible and occur at $E_{\text{pc}} = -0.41$ V for **3b** and $E_{\text{pc}} = -0.77$ V for **4**. On a reverse, oxidative scan, there is evidence for reoxidation at $E_{\text{pa}} = -0.20$ V for **3b** and at $E_{\text{pa}} = -0.68$ V for **4**. There is no sign of additional product waves in the voltammograms after reduction. A reduction wave for *trans*- $[\text{Os}^{\text{II}}(\text{tpy})(\text{Cl})_2(\text{NS})]^+$ at $E_{1/2} = -0.30$ V has been reported under the same experimental conditions.⁶ The reduction waves appear to be thionitrosyl ligand-based reductions. Analogous waves have been reported for $\text{Os}^{\text{II}}\text{-NO}$ complexes.²³

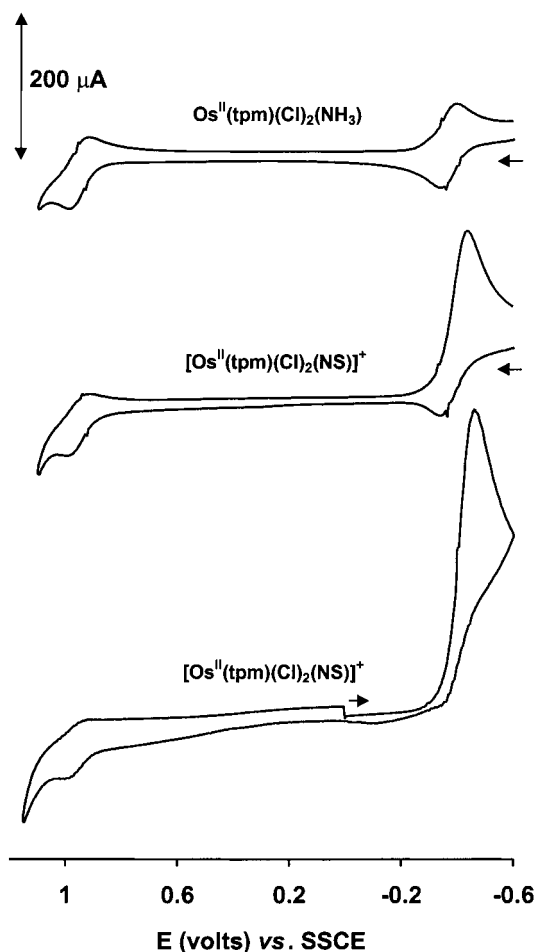
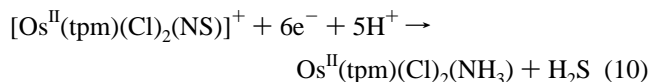


Figure 5. Cyclic voltammograms of $[\text{Os}^{\text{III}}(\text{tpm})(\text{Cl})_2(\text{NH}_3)](\text{PF}_6)$ (**6**) and $[\text{Os}^{\text{II}}(\text{tpm})(\text{Cl})_2(\text{NS})](\text{PF}_6)$ (**3b**) in 3 M HCl. Glassy carbon disk working electrode at 200 mV/s vs SSCE.

Cyclic voltammograms of $[\text{Os}^{\text{II}}(\text{tpm})(\text{Cl})_2(\text{NS})]^+$ (**3b**) and $[\text{Os}^{\text{III}}(\text{tpm})(\text{Cl})_2(\text{NH}_3)]^+$ (**6**) in 3 M HCl are shown in Figure 5. For **6**, reversible waves for the $\text{Os}^{\text{III}}/\text{Os}^{\text{II}}$ and $\text{Os}^{\text{IV}}/\text{Os}^{\text{III}}$ couples appear at $E_{1/2} = -0.36$ and $+0.95$ V vs SSCE, respectively as reported earlier for $[\text{Os}^{\text{III}}(\text{tpm})(\text{Cl})_2(\text{NH}_3)]^+$ prepared by another route.¹² In a solution containing **3b**, an initial reductive scan reveals a multi-electron wave at $E_{\text{pc}} = -0.47$ V. Upon scan reversal, waves for the $\text{Os}^{\text{III}}/\text{Os}^{\text{II}}$ and $\text{Os}^{\text{IV}}/\text{Os}^{\text{III}}$ couples of $\text{Os}^{\text{II}}(\text{tpm})(\text{Cl})_2(\text{NH}_3)$ are observed. On the basis of these results, electrochemical reduction of **3b** occurs by



In voltammograms of DMSO solutions containing $\text{Os}^{\text{III}}(\text{tpm})(\text{Cl})_2(\text{NSO})$ (**7**), a reversible $\text{Os}^{\text{III}}/\text{Os}^{\text{II}}$ couple appears at $E_{1/2} = -0.40$ V vs SSCE. On the oxidative side, an irreversible $\text{Os}^{\text{III}} \rightarrow \text{Os}^{\text{IV}}$ wave appears at $E_{\text{pa}} = +0.90$ V.

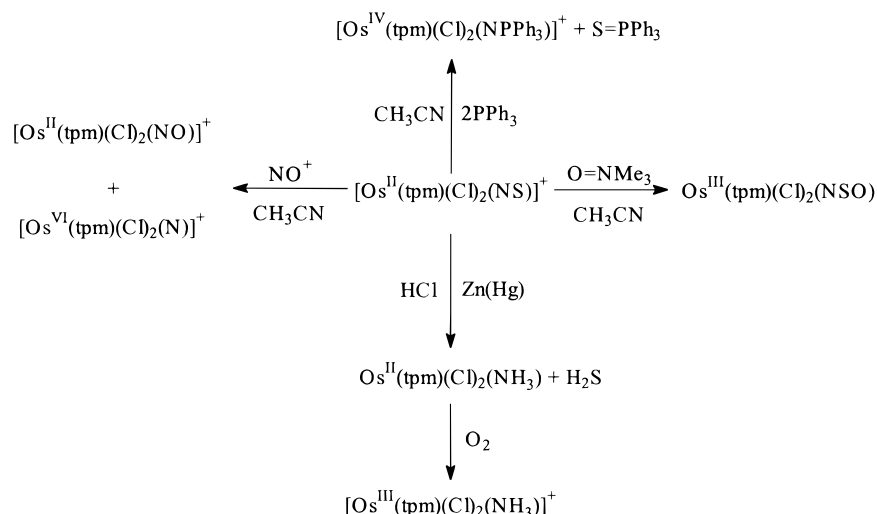
Discussion

The synthetic procedure for preparation of Os^{II} thionitrosyl complexes is based on the formation of the unstable 5-thio-1,2,3,4-thiazololate ring anion, CS_2N_3^- , which is known to decompose to give SCN^- , N_2 , and S^0 .²⁴ In the presence of nitridos **1** or **2**, nucleophilic attack on $\text{Os}^{\text{VI}}\equiv\text{N}$ by the thiolato portion of the ring takes place with sulfur atom transfer. This

(22) Williams, D. S.; White, P. S.; Meyer, T. J. *J. Am. Chem. Soc.* **1995**, *117*, 823.

(23) (a) Murphy, W. R., Jr.; Takeuchi, K. J.; Meyer, T. J. *J. Am. Chem. Soc.* **1982**, *104*, 517; (b) Pipes, D. W.; Meyer, T. J. *Inorg. Chem.* **1984**, *23*, 2466; (c) Ooyama, D.; Nagao, H.; Ito, K.; Nagao, N.; Howell, F. S.; Mukaida, M. *Bull. Chem. Soc. Jpn.* **1997**, *70*, 2141.

Scheme 1



is accompanied by reduction of Os^{VI} to Os^{II} and formation of the corresponding thionitrosyl complexes **3** or **4**.⁷

Several Os^{II} thionitrosyl complexes have been characterized by infrared measurements.⁵ The usual range for $\nu(\text{N}=\text{S})$ is 1400–1150 cm⁻¹, and $\nu(\text{N}=\text{S})$ for **3b** and **4** at 1317 and 1288 cm⁻¹ fall into this range. For comparison, $\nu(\text{N}=\text{S})$ appears at 1310, 1295, and 1270 cm⁻¹ in Os(NS)(Cl)₃(PPh₃)₂,^{5a} *trans*-[Os(NS)(Cl)₂(tpy)]⁺,⁶ and Os(NS)(Cl)(OEP)²⁵ (OEP = 2,3,7,8,12-,13,17,18-octaethylporphyrinato anion).

Low-intensity bands for **3b** and **4** appear in the region 540–420 cm⁻¹ which shift ~15 cm⁻¹ in ¹⁵N-labeled complexes. A related series of bands appear at 495, 454, and 221 cm⁻¹ for [Os(NS)(NSCl)(Cl)₄]⁻ which have been assigned to the normal modes $\nu_s(\text{Os}-\text{N})$, $\nu_{as}(\text{Os}-\text{N})$, and $\delta(\text{Os}-\text{NS})$.²⁶

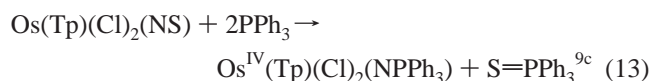
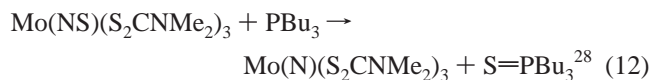
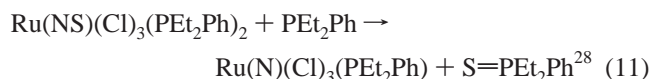
As shown in Figure 4, two bands of low absorptivity appear in the visible for both **3b** and **4**. In a molecular orbital scheme, with the Os–NS bond axis defined as *z*, $d\pi-\pi^*(\text{NS})$ mixing is dominated by d_{xz} and d_{yz} with the d_{xy} (in-plane) orbital orthogonal to the dominant interaction. Based on this orbital scheme, the visible bands can be assigned to the transitions $d_{xy}\rightarrow\pi_1^*$ and $d_{xy}\rightarrow\pi_2^*$. The splitting between these bands of 7400 cm⁻¹ is a consequence of low symmetry and spin–orbit coupling at Os. Related low-intensity bands have been reported for *cis*- and *trans*-[Os^{II}(tpy)(Cl)₂(NO)]⁺ at 480 nm ($\epsilon = 120 \text{ M}^{-1} \text{ cm}^{-1}$) and 575 nm ($\epsilon = 250 \text{ M}^{-1} \text{ cm}^{-1}$).²²

The Os–N(thionitrosyl) bond lengths are 1.780(14) Å for **3c** and 1.800(8) Å for **4**. They fall in the range 1.731(4)–1.834(7) Å for Os^{II} thionitrosyl complexes,^{5c} consistent with sp hybridization with the NS ligand is treated as a 3-electron donor. The multiple bond character of the Os–N bond is in agreement with the short Os–N bond distances. The N–S bond lengths of 1.489(15) and 1.493(8) Å for **3c** and **4** and are comparable to bond distances in other thionitrosyl complexes.^{5e,7,26} The N–S bond lengths are also consistent with largely NS⁺ character by comparison with the NS⁺ cation in which the N–S bond length

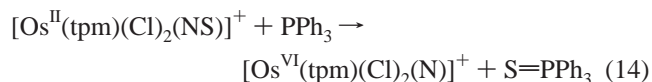
is 1.495 Å.²⁷ The Os–N–S bond angle is almost linear at 179.3(9)° in [Os^{II}(tpm)(Cl)₂(NS)]⁺ and at 166.9(9)° in Os^{II}(Tp)(Cl)₂(NS). The Os–N(Tp) bond lengths *cis* to NS are 2.086(5)° and 2.066(6)°, while the *trans* bond length is 2.125(5)° consistent with a *trans* effect exerted by the thionitrosyl ligand. In [Os^{II}(tpy)(Cl)₂(NS)]⁺,⁷ the Os–N(tpy) bond distance *trans* to NS is 2.032(7) Å. It is 2.079(7) Å for *cis*. This difference is a characteristic feature of the structural chemistry of metal–terpyridine complexes and the strained metal–terpyridine coordination.^{6,8,22}

Reactivity. A summary of the thionitrosyl reactions documented here is given in Scheme 1. These results reveal a versatile and extensive redox chemistry of the thionitrosyl group in [Os^{II}(tpm)(Cl)₂(NS)]⁺.

The reaction between [Os^{II}(tpm)(Cl)(NS)]⁺ (**3b**) and PPh₃ (eq 3) reveals the ability of the NS group to transfer a S atom to PPh₃. There is a well-precedented reactivity, examples being



The results of the kinetic study reveal that S-atom transfer is facile. The mechanism presumably involves initial S-atom transfer,



followed by attack of a second PPh₃ on the intermediate nitrido complex. This reaction is known to be rapid.

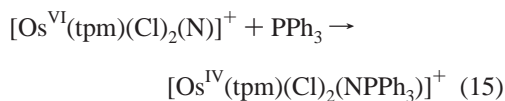
(24) (a) Lieber, E.; Pillai, C. N.; Ramachandran, J.; Hites, R. D. *J. Org. Chem.* **1957**, *22*, 1750. (b) Lieber, E.; Oftedahl, E.; Reo, C. N. *R. J. Org. Chem.* **1963**, *28*, 194. (c) Browne, A. W.; Hoel, A. B.; Smith, G. B. L.; Swezey, F. h. *J. Am. Chem. Soc.* **1923**, *45*, 2541. (d) *Carbon Disulphide in Organic Chemistry*; Dunn, A. D., Rudolf, W.-D., Eds.; Ellis Horwood Ltd.: New York, 1989.

(25) Cheng, L.; Chen, L.; Chung, H.-S.; Khan, M. A.; Richter-Addo, G. B.; Young, V. G., Jr. *Organometallics* **1998**, *17*, 3853.

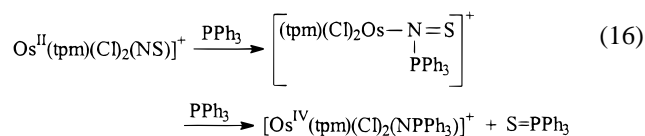
(26) Weber, R.; Müller, U.; Dehnicke, K. *Z. Anorg. Allg. Chem.* **1983**, *504*, 13.

(27) Barrow, R. F.; Warm, R. J.; Fitzgerald, A. G.; Fyoffe, B. D. *Trans. Faraday Soc.* **1964**, *60*, 294.

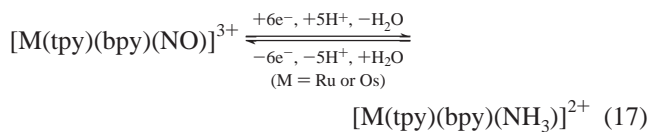
(28) Bishop, M. W. Chatt, J.; Dilworth, R. J. *J. Chem. Soc., Dalton Trans.* **1979**, 1.



When discussed in this way, the reaction with PPh_3 infers a S-atom reactivity for bound NS consistent with the expected $\text{N}^{\delta-} \equiv \text{S}^{\delta+}$ electronic distribution in bound NS^+ . An alternate mechanism, which we cannot rule out, would involve rate-limiting attack on N, followed by S-atom transfer.

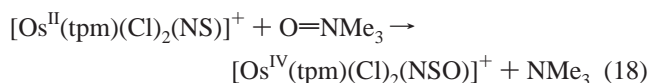


With added amalgamated zinc as reductant in 3 M HCl, the sulfur atom undergoes a net reduction according to eq 6 to give $\text{Os}^{\text{II}}-\text{NH}_3$ followed by O_2 oxidation to $\text{Os}^{\text{III}}-\text{NH}_3^+$. This reaction is analogous to the known reduction of nitrosyl to ammine under reducing conditions in polypyridyl complexes of ruthenium and osmium in which nitrosyl-ammine interconversion is reversible.²³

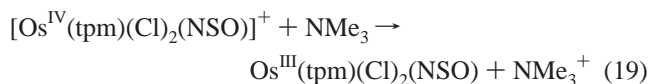


Reduction of the nitrosyl ligand in these complexes has been proposed to occur by a series of stepwise intermediates, $[\text{Os}(\text{tpy})(\text{bpy})(\text{NHO})]^{2+}$, $[\text{Os}(\text{tpy})(\text{bpy})(\text{NH}_2\text{O})]^{2+}$, $[\text{Os}(\text{tpy})(\text{bpy})(\text{NH}_2\text{OH})]^{2+}$, and reduction of thionitrosyl may follow an analogous course.

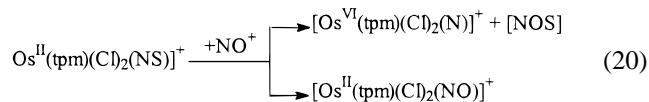
The reaction between $[\text{Os}^{\text{II}}(\text{tpm})(\text{Cl})_2(\text{NS})]^+$ (**3b**) and trimethylamine *N*-oxide reveals that the S atom can also be oxidized by O-atom transfer from *N*-oxides with formation of $\text{Os}^{\text{III}}\text{NSO}$. There are several metal-thiazato complexes in the literature. Examples in Os chemistry include formation of $\text{Os}(\text{NSO})(\text{X})_2(\text{PPh}_3)_2$ (X = Cl, Br) by reaction of sulfur with $\text{Os}(\text{NO})(\text{X})_3(\text{PPh}_3)_2$ in benzene.^{6c} There are also examples of metal-thiazato formation by oxidation of metal-thionitrosyl complexes by dioxygen.^{19d} The example found here appears to be the first which utilizes an *N*-oxide reagent. The initial step presumably involves O-atom transfer and formation of Os^{IV} as an intermediate.



On the basis of the electrochemical measurements, Os^{IV} is a powerful oxidant in this coordination environment and once formed, is presumably reduced to Os^{III} by released NMe_3 .

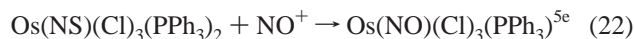
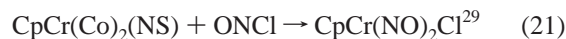


The last reaction investigated was between $[\text{Os}^{\text{II}}(\text{tpm})(\text{Cl})_2(\text{NS})]^+$ (**3c**) and NO^+ in CH_3CN . In this case, there are two products, the nitrido complex, $[\text{Os}^{\text{VI}}(\text{tpm})(\text{Cl})_2(\text{N})]^+$, and the nitrosyl complex, $[\text{Os}^{\text{II}}(\text{tpm})(\text{Cl})_2(\text{NO})]^+$, in a ratio of $\sim 4:1$. Based on the products, there appears to be a competition between NO^+/NS^+ exchange and NO^+ attack on the S atom of the thionitrosyl ligand although we have no evidence for $[\text{NOS}]^+$ or the products of its further reactions.



On the basis of the labeling study, which utilized $[\text{Os}^{\text{II}}(\text{tpm})(\text{Cl})_2(^{15}\text{NS})]^+$, the N atom of the nitrosyl originates in NO^+ . The suggestion of competitive attack on sulfur is based on the appearance of the Os^{VI} nitrido complex as a product. This is an interesting reaction in that extraction of S occurs to give back the starting nitrido complex.

NO^+/NS^+ exchange in transition metal thionitrosyls is also known in the literature. Examples include



Conclusions

The results of the reactivity studies provide an interesting comparison with related nitrosyls. The redox chemistry of the nitrosyl group in the relatively electron deficient coordination environment of polypyridyl complexes is dominated by nucleophilic attack at the coordinated N atom. In the case of the thionitrosyl ligand there is a different internal electronic distribution in which the S atom is relatively electron deficient. Reaction with PPh_3 or NO^+ results in S-atom transfer and reformation of the starting nitrido complex. The thionitrosyl ligand can also be oxidized further as shown by the reaction with trimethylamine *N*-oxide. Finally, both the coordinated nitrosyl and thionitrosyl ligands share the ability to undergo reduction under acidic conditions to give coordinated ammonia.

Acknowledgment is made to the National Science Foundation under Grant No. CHE-9503738 for support of this research. E.-S.E.-S. thanks the Egyptian Government for the data collection Grant. We also thank Drs. James M. Mayer and Thomas J. Crevier at the University of Washington for sharing results prior to publication and interesting discussions.

Supporting Information Available: Portions of infrared spectra with isotopic shifts for **3b**, **4**, **3b***, and **4** in the regions 1350–1200 and 540–420 cm^{-1} ; cyclic voltammogram of the product of the reaction between **3c** and NO^+ , additional details of the crystallographic analysis of the compounds **3c** and **4**, fully labeled ORTEP diagrams; and tables of atomic coordinates, isotropic thermal parameters and bond distances and angles. This material is available free of charge via the Internet at <http://pubs.acs.org>.

IC981449K

(29) Greenhough, T. J.; Kolthammer, B. W. S.; Legzdins, P.; Trotter, J. *Inorg. Chem.* **1979**, *18*, 3548.